Solid-State Electronics Vol. 35, No. 5, pp. 699–704, 1992
Printed in Great Britain.

0038-1101/92 $5.00 + 0.00

INFLUENCE OF MAJORITY CARRIER BANDTAILS ON THE PERFORMANCE OF SEMICONDUCTOR DEVICES

P. VAN MIEGHEM, S. DECOUTERE, G. BORGHS and R. MERTENS
Interuniversity Micro Electronics Center (IMEC), Kapeldreef 75, B-3001 Leuven, Belgium

(Received 10 April 1991; in revised form 25 August 1991)

Abstract—A model for bandtailing is built into the 1-D device simulator SEDAN. The influence of bandtails on the current gain of a state-of-the-art bipolar transistor is examined. It is shown that for transistors with high emitter doping, bandtail effects decrease the current gain significantly. This reduction in current gain is more pronounced at low temperature.

NOTATION

a_B	effective Bohr radius (cm)
β	current gain
β_1	current gain calculated with bandtailing
ΔE_g	bandgap narrowing (BGN) (eV)
$\Delta E_{g,\text{many-body}}$	BGN due to many-body interactions (eV)
$\Delta E_{g,\text{tail}}$	BGN due to bandtailing (eV)
ϵ	the permittivity in the semiconductor ($F\,cm^{-1}$)
$E_{c(v)}$	conduction (valence) band energy (eV)
E_g	bandgap energy (eV)
f_T	cutoff frequency where $\beta = 1$
κ	inverse screening length (cm^{-1})
L_p	hole diffusion length (cm)
m	effective mass times electron mass (kg)
$M_0(E)$	integrated unperturbed DOS (cm^{-3})
$\mu_{pE(nB)}$	the minority carrier mobility in the emitter (base) ($cm^2V^{-1}s^{-1}$)
$N_{c(v)}$	effective density of states in conduction (valence) band (cm^{-3})
$N_{E(B)}$	emitter (base) doping concentration (cm^{-3})
n_{ie}	effective intrinsic carrier concentration (cm^{-3})
n_{i0}	intrinsic carrier concentration (cm^{-3})
$\rho_0(E)$	unperturbed density of states (DOS) ($eV^{-1}\,cm^{-3}$)
σ	root mean square of the potential energy fluctuation due to the random distribution of impurities (eV)
τ_E	emitter time delay (s)
τ_{EC}	total time delay (from emitter to collector) (s)
V_{β}	emitter–base voltage for which β achieves its maximum (V)
V_{be}	emitter–base voltage (V)
$x_{E(B)}$	the emitter (base) width (cm)
$\zeta_{n(p)}$	quasi-Fermi levels for electrons (holes) (eV)

1. INTRODUCTION

Heavy doping effects may influence device operations considerably. These heavy doping effects result from different physical mechanisms. Many-body effects (mainly electron–electron and electron–impurity interactions) contribute most dominantly. Besides a shift of the energy levels leading to bandgap narrowing (BGN), electron–electron interactions also weakly deform the density of states (DOS) from its unperturbed distribution[1]. Apart from a slight shrinking of the bandgap, the electron-impurity scattering[2] modifies the DOS more significantly and causes states that tail into the energy gap. Along with these many-body effects, the random distribution of impurities merely distorts the DOS[3] by creating significant bandtails. Since its nature is statistical, the description differs from many-body effects. In this work, supposing that the many-body influences are known, we concentrate on the latter effect and refer to it as bandtailing.

By now, BGN is recognized to exert an important influence on device performance[4]. It is generally included in device simulators, most often by an empirical model (such as the Slotboom formula[5] in Si). On the other hand, bandtailing is usually neglected because its repercussion on device performance is smaller than BGN. Above all, the physical description of bandtailing is cumbrous to plug into a device simulator since the tailed DOS functions need additional numerical integrations which blow up computer time.

In this article, we propose an efficient numerical method to include bandtailing for *majority carriers* in a device simulator. The model [see eqn (6)] is programmed into SEDAN[6]. This built-in into SEDAN hardly increases the simulation time. The current gain β of a state-of-the-art high-speed Si bipolar transistor with an f_T of 40 GHz[7] is examined. At very high doping concentration or low temperatures, this effect of band tailing is demonstrated to be sufficiently pronounced to influence characteristics of semiconductor devices.

2. A MODEL FOR BANDTAILING

Detailed numerical simulations for devices can be split up into two classes[8] corresponding to the physical models they are based on. The first class uses conventional (or empirical) device physics (CDP) while the second class starts from first-principles. The latter determines the number of carriers from an intricate tailed DOS function, which itself is

function of the number of carriers n through screening effects[3]. This calculation clearly needs self-consistent numerical procedures and hence, a lot of computer time. We have preferred a less arduous way and propose a CDP approach.

The effect of bandtailing is modeled as an equivalent downward shift of the Fermi level while using a parabolic DOS instead of a DOS distortion. This is illustrated in Fig. 1. It means that the effect of tailing introduces a supplementary narrowing of the bandgap besides the many-body BGN effect and forms a part of the total bandgap shrinkage ΔE_g:

$$\Delta E_g = \Delta E_{g,\text{many-body}} + \Delta E_{g,\text{tail}} \tag{1}$$

Although this separation is an approximation, it can be justified theoretically[9] but presents a more complete description because nearly all theories of BGN assume a parabolic DOS and neglect bandtailing. Further, we have followed a semiclassical approach, which is shown[9] to be very appropriate in describing the number of majority carriers in a degenerate semiconductor, to deduce values for $\Delta E_{g,\text{tail}} = E_{F0} - E_{Ft}$. Assuming complete ionization, both introduced Fermi levels are easily calculated from the impurity concentration N, preserving electrical neutrality, as:

$$N = n_{el} = \int_{-\infty}^{\infty} \rho(E) f_{FD}(E - E_{Ft})\,dE = \int_{0}^{\infty} \rho_0(E) f_{FD}(E - E_{F0})\,dE, \tag{2}$$

where E_{Ftn} denotes the Fermi level using the tailed distribution $\rho(E)$, whereas E_{F0n} equals the Fermi level for the unperturbed DOS $\rho_0(E)$, and $f_{FD}(E)$ is the Fermi–Dirac function. The solution for $\Delta E_{g,\text{tail}}$ from (2) in the semiclassical approach:

$$\Delta E_{g,\text{tail}} = \frac{e^2}{\epsilon \kappa^2} \frac{1}{\sqrt{\pi}} \int_0^{\infty} dt M_0(\sqrt{2}\sigma t) \exp(-t^2), \tag{3}$$

where

$$M_0(E) = \int_0^E \rho_0(t)\,dt, \tag{4}$$

$$\sigma = \frac{e^2}{\epsilon} \sqrt{\frac{n}{8\pi\kappa}}, \tag{5}$$

in which κ denotes the inverse screening length and ϵ the permittivity in the semiconductor, which is derived in Ref. [9].

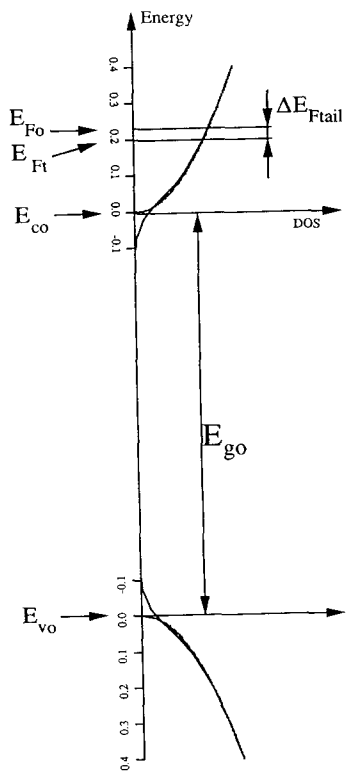

Fig. 1. Bandtailing causes the Fermi level E_{Ft} to lie below the Fermi level E_{F0} of the corresponding parabolic DOS for a same amount of carriers n. The picture is drawn to scale for Si. (Energy in eV.)

This semiclassical approach[9] for formula (3) gives a good estimate of the real Fermi level shift which is directly applicable for device simulators. Indeed, we have calculated the maximal relative error by comparing the semiclassical method with Sayakanit's path integral approach[10], which practically coincides with the Halperin and Lax theory[11] in the deep energy tail. We prefer Sayakanit's approach over that of Halperin and Lax since it offers an more elegant and precise way to define the relative error. As the semiclassical method overestimates the number of deep tail states, we have compared this overestimated number to the number of tail states under the band edge and defined this ratio as the relative error. To find the excess of deep tail states, the number of states according to both the Kane and Sayakanit DOS are computed at the point where Sayakanit's DOS crosses the Kane-DOS (as proposed by Sayakanit[10]). This measure for the relative error is an upper boundary because the overestimated number is related to the number of tail states rather than to the total number of carriers. The semiclassical formula (3) assumes that the Fermi level lies in the conduction band implying that the total number of carriers exceeds that of the tail states. We obtain that the maximal relative error never exceeds 28% for the doping concentrations covered in Fig. 2 and decreases towards higher doping concentrations, as it should because the semiclassical method describes the exact high-density limit[9]. Just as the band tail effect becomes negligible, the semiclassical formula (3) overestimates the tail contribution, but gains accuracy for increasing doping concentrations, where band tails affect semiconductor properties. In com-

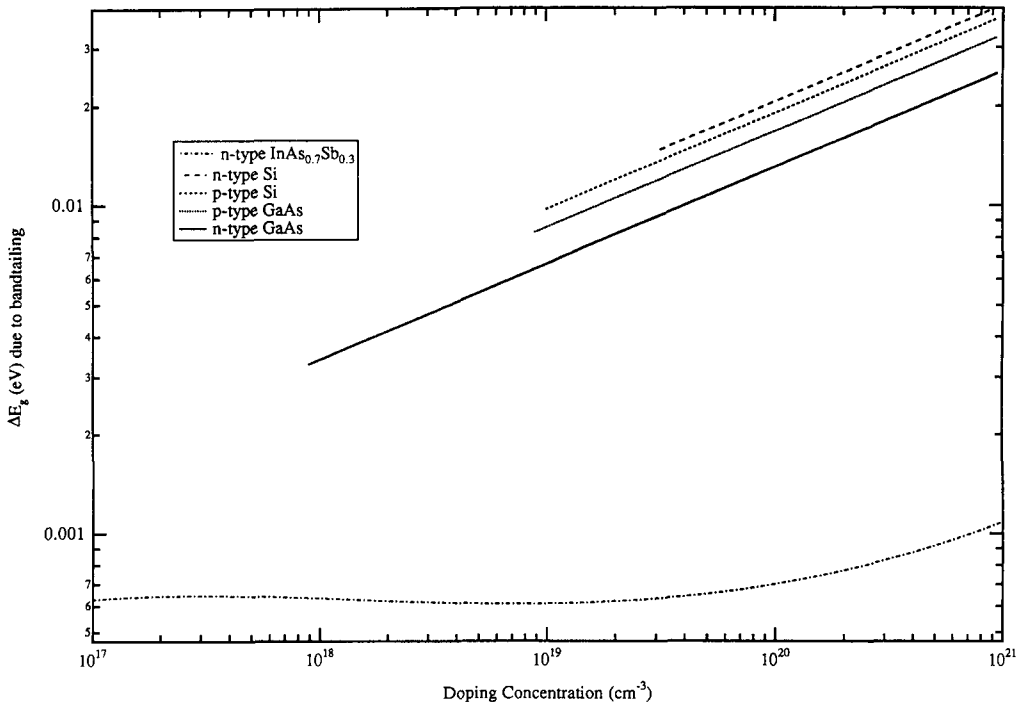

Fig. 2. The Fermi level shift $\Delta E_{g,tail}$ as a function of doping concentration for semiconductors with a parabolic unperturbed DOS (Si, GaAs) and a non-parabolic unperturbed DOS ($InAs_{0.3}Sb_{0.7}$). The semiclassical model is only valid when the Fermi level lies in the conduction (n-type) or valence band (p-type). The curves are only drawn for doping concentrations above this validity threshold.

parison with other approximate models (e.g. for mobility, lifetime, etc.) in a device simulator and in view of its elegance built-in into a device simulator, we believe that the use of this formula (3) is well-justified.

If the unperturbed DOS is a simple square root of energy (as for Si and GaAs), expression (3) simplifies considerably, yielding:

$$\Delta E_{g,tail} = 0.041078 \frac{m^{3/2} e^2 \sigma^{3/2}}{\epsilon \hbar^3 \kappa^2} \tag{6}$$

with

$$\kappa = \frac{2}{\sqrt{a_B}} \left(\frac{3n}{\pi} \right)^{1/6} \tag{7}$$

and where $a_B = 4\pi\epsilon\hbar^2/me^2$ denotes the effective Bohr radius and m is the effective mass.

The dependence of $\Delta E_{g,tail}$ on doping concentration is shown in Fig. 2 for Si and GaAs together with $InAs_{0.3}Sb_{0.7}$ which exhibits a strong non-parabolic unperturbed DOS. It is observed that $\Delta E_{g,tail}$ is substantial for Si and GaAs at high doping concentrations, which are typical for emitters of advanced bipolar transistors. Moreover, the vertical scaling to obtain high cutoff frequencies tends to increase the doping concentration in the base resulting in growing importance of bandtailing in calculating collector current densities.

3. SEDAN SIMULATION

The influence of bandtailing on device performance is illustrated for an Si bipolar transistor[7] for which the doping profile is drawn in Fig. 3. The emitter and base are heavily doped. The influence of bandtailing on the current gain of this transistor[12] is studied because of the high sensitivity of current gain for changes in bandgap energy. The simulations were performed using identical parameters for both the model with bandtailing (6) and without bandtailing. In the latter case only BGN ($\Delta E_{g,many\text{-}body}$) is included.

For homogeneous emitter and base doping profiles, the maximum of the current gain β_{max} is approximately described by[13]:

$$\beta_{max} \approx \beta_0 \frac{n_{ieB}^2}{n_{ieE}^2}, \tag{8}$$

where

$$\beta_0 = \frac{N_E x_E \mu_{nB}}{N_B x_B \mu_{pE}}, \tag{9}$$

with $N_{E(B)}$ the emitter (base) doping concentration, $x_{E(B)}$ the emitter (base) width and $\mu_{pE(nB)}$ the minority carrier mobility in the emitter (base). The derivation of (8) assumes the evaluation of the p–n-product close to the ohmic contacts, where $\zeta_n = \zeta_p$. The

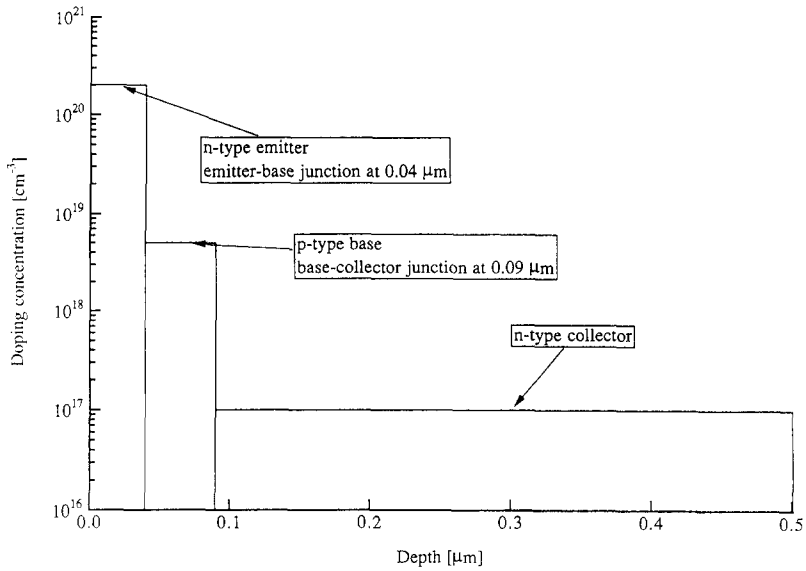

Fig. 3. Doping profile of the bipolar transistor studied.

effective intrinsic carrier concentration, $n_{ie}^2 = np$, can be worked out further. Defining[14]:

$$R_{c(v)}(y) = N_{c(v)} \int_{-\infty}^{\infty} g_{c(v)}(x) \frac{dx}{1+\exp(x-y)}, \quad (10)$$

where $g_{c(v)}(x) = kT/N_{c(v)}\,\rho_c(kTx)$, with $\rho_c(E)$ the density of states in the conduction band, we obtain:

$$np = N_c N_v R_v\left(\frac{E_v - \zeta_p}{kT}\right) R_c\left(\frac{\zeta_n - E_c}{kT}\right), \quad (11)$$

where $\zeta_{n(p)}$ is the quasi-Fermi level for the electrons (holes).

Consider the n–p product in the emitter. Since holes are minority carriers, the asymptotic expression for:

$$R_v(y) = A_v e^y, \quad (12)$$

where

$$A_v = \int_{-\infty}^{\infty} g_v(u) e^{-u}\, du, \quad (13)$$

yields an excellent approximation and (11) reduces to:

$$np \approx A_v N_c N_v \exp\left(\frac{E_v - \zeta_p}{kT}\right) R_c\left(\frac{\zeta_n - E_c}{kT}\right). \quad (14)$$

Writing $E_v = E_c + E_g + \Delta E_g$ and invoking the definition of the intrinsic carrier concentration, (14) reads:

$$np = A_v n_{i0}^2 \exp\left(\frac{\Delta E_g}{kT}\right) \exp\left(\frac{E_c - \zeta_p}{kT}\right) R_c\left(\frac{\zeta_n - E_c}{kT}\right). \quad (15)$$

The voltage for which the current gain achieves its maximum does not belong to the high injection region and, hence, to a good approximation, we may suppose that the number of electrons equals the donor concentration, or:

$$\frac{E_c - \zeta_n}{kT} = R_c^{-1}\left(\frac{N_E}{N_c}\right), \quad (16)$$

where $y = R^{-1}(x)$ denotes the solution of $x = R(y)$. Substituting (16) into (15) and recalling that $\zeta_n = \zeta_p$, we finally arrive at:

$$np = A_v n_{i0}^2 \exp\left(\frac{\Delta E_g}{kT}\right) \exp\left[-R_c^{-1}\left(\frac{N_E}{N_c}\right)\right] \frac{N_E}{N_c}, \quad (17)$$

which is modeled in Sedan3, invoking (6) as:

$$np = n_{i0}^2 \exp\left(\frac{\Delta E_g + \Delta E_{gt}}{kT}\right) \exp\left[-F_{1/2}^{-1}\left(\frac{N_E}{N_c}\right)\right] \frac{N_E}{N_c}, \quad (18)$$

where $F_{1/2}(y)$ is the Fermi–Dirac integral of order 1/2.

Plugging (18) into (8), we get the approximate formula for β_{max}:

$$\beta_{max} \approx \beta^* \exp\left(\frac{-\Delta E_{gE} - \Delta E_{gtE} + \Delta E_{gB} + \Delta E_{gtB}}{kT}\right), \quad (19)$$

where

$$\beta^* = \frac{N_E^2 N_v x_E \mu_{pE}}{N_B^2 N_c x_B \mu_{nB}} \exp\left[-F_{1/2}^{-1}\left(\frac{N_E}{N_c}\right) + F_{1/2}^{-1}\left(\frac{N_B}{N_v}\right)\right]. \quad (20)$$

However, the approximate relation (19) should never be used to extract real values for bandtailing from transistor measurements because the accuracy needed to determine BGN and bandtailing far exceeds the accuracy of (8). This simple model, here, is adopted to explain tendencies observed from the simulations. We prefer to investigate the difference in current gain $\Delta\beta = \beta - \beta_t$ rather than β_t/β, because the latter does not reach a maximum in the interval [0.5 V, 1 V].

Both β and β_t are drawn in Fig. 4 for several emitter doping concentrations, varying from 10^{20} to $5\,10^{20}\,cm^{-3}$, holding all other doping profile parameters fixed. The influence of tailing is predominant for emitter doping concentrations above $10^{20}\,cm^{-3}$ as is observed from Fig. 4. The maximum difference in current gain increases strongly with emitter doping N_E. The corresponding pictures for a variable base

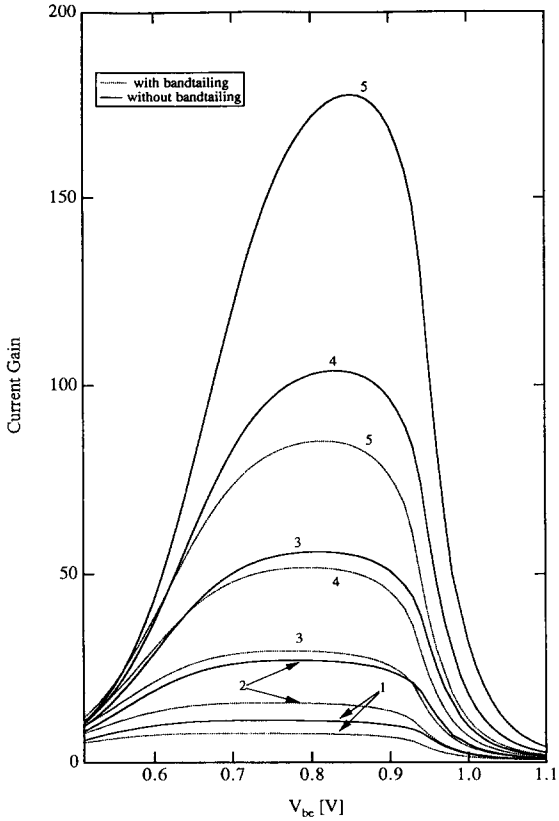

Fig. 4. The current gain β and β_t vs emitter–base voltage and at zero collector–base voltage for variable emitter doping concentrations N_E. Both curves for β and β_t expand for increasing $N_E = 10^{20}$–$5 \times 10^{20}\,cm^{-3}$. The emitter doping concentration N_E is shown in units of $10^{20}\,cm^{-3}$.

doping N_B, ranging from 10^{18} to $10^{19}\,cm^{-3}$, are shown in Fig. 5. For the lowest base concentration $N_B = 10^{18}\,cm^{-3}$, β peaks at low values of V_{be} because the transistor is operated near punchthrough. The decrease in $\Delta\beta_{max}$ with base doping is explained by (19) because the sign of ΔE_{gtB} is opposite to that of ΔE_{gtE}. The $\Delta\beta_{max}$ extracted from Figs 4 and 5 does not show a simple dependence on doping concentration, a feature expected from (19).

The most important limiting factor in the temperature dependence of the current gain of a BJT is bandgap narrowing[15]. The effect of bandtailing on the temperature dependence of the current gain is demonstrated in Fig. 6. Especially at low temperature, bandtailing has a dramatic influence. The difference $\Delta\beta$ is a weakly decreasing function of temperature. The maximum difference in current gain is best fitted as $\Delta\beta_{max}(T) \approx 18.9\,T^{-0.08}$ for the temperature range varying from 150 to 500 K. In conclusion, besides the already strong effect of BGN on the current gain at low temperature, the effect of bandtailing decreases β even faster. This pronounced degradation in current gain at low temperature is of special interest since bipolar transistors have an attractive power delay product at low temperatures[16].

From the simulations (see Figs 4–6), a shift of β_t to lower base–emitter voltages is observed. If the voltage corresponding to the maximum current gain V_β is considered, the difference $\Delta V_\beta = V_\beta - V_{\beta t}$ turns out to be roughly of the order of $\Delta E_{gtE} + \Delta E_{gtB}$. However, no simple formula to evaluate this shift ΔV_β is available because V_β strongly depends, apart from the lifetime, on the dominance of punchthrough or high injection. In addition, Sedan3 is not well-suited to study this small difference in detail.

The influence of bandtailing on f_T of the studied bipolar transistor (Fig. 3) can be estimated from arguments outlined by De Man *et al.*[17]. They have demonstrated that the total time delay τ_{EC} is modified by BGN through the emitter delay time τ_E. For constant doping profiles, τ_E reads[18]:

$$\tau_E = \frac{K}{\beta}, \tag{21}$$

$$K = \tau_r\left\{1 - \left[\cosh\left(\frac{x_E}{L_p}\right) + \frac{L_p}{\tau_r s}\sinh\left(\frac{x_E}{L_p}\right)^{-1}\right\}, \tag{22}$$

where τ_r is the recombination lifetime in the bulk and s the recombination velocity at the emitter contact,

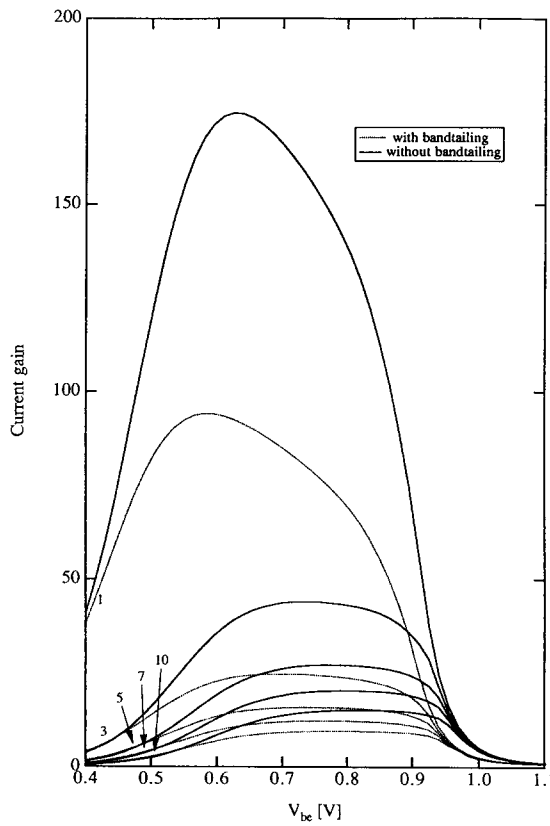

Fig. 5. The current gain β and β_t vs emitter–base voltage and at zero collector–base voltage for variable base doping concentrations N_B. Both curves for β and β_t decline for increasing $N_B = 10^{18}$–$10^{19}\,cm^{-3}$. The base doping concentration N_B is shown in units of $10^{18}\,cm^{-3}$.

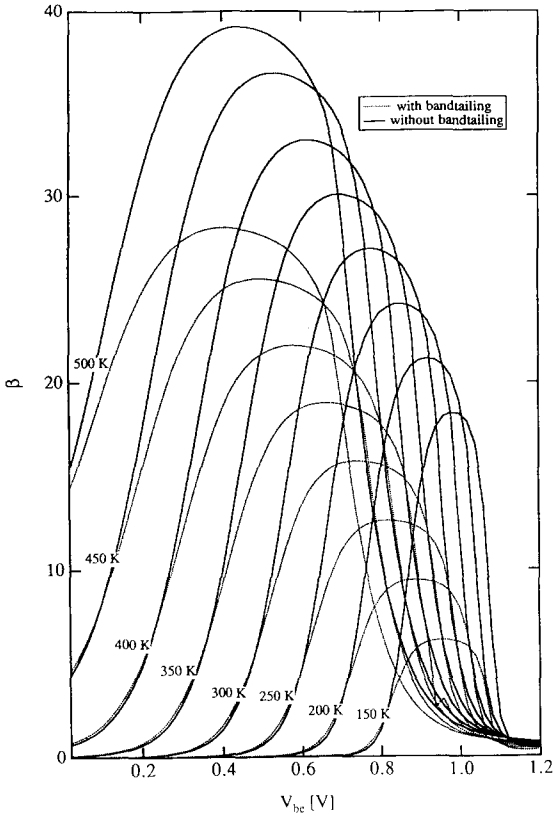

Fig. 6. Both current gain β and β_i vs emitter–base voltage and at zero collector–base voltage for various temperatures.

which simplifies for a short (transparent) emitter ($x_E \ll L_p$) to:

$$K = \frac{x_E}{s} + \frac{x_E^2}{2D_p}. \tag{23}$$

Consequently, when neglecting the weak dependence of K on ΔE_g, we obtain:

$$\frac{\delta}{\delta \Delta E_{gt}}\left(\frac{1}{f_T}\right) = 2\pi K \frac{\delta}{\delta \Delta E_{gt}}\left(\frac{1}{\beta}\right), \tag{24}$$

or the sensitivity of $1/f_T$ for bandtailing is proportional to the sensitivity of the inverse of current gain for bandtailing. Thus, to first-order, the effects of bandtailing on the f_T of a bipolar transistor with constant doping profiles are similar to the tendencies observed in β.

At last, we recall that the real effect of bandtailing may be more pronounced than demonstrated here because our simulation did not include the influence of bandtailing on mobility, lifetime nor the diffusion coefficient. The physics of heavy doping behind these parameters, however, is still not well understood[19].

4. CONCLUSION

The influence of bandtail effects on the current gain of a bipolar transistor is shown to be substantial for high emitter doping concentrations and low temperatures. As future semiconductors device design tends towards further vertical scaling for improved cutoff frequencies (leading to still higher doping concentrations), the bandtail effect should be included in the simulations. Beside this work on the influence of the effective intrinsic carrier concentration, a thorough study of bandtailing on minority carrier mobility, lifetime and diffusion coefficients is needed.

Acknowledgements—The authors would like to thank L. Dupas for his assistance in programming the model into Sedan3. Fruitful discussions with J. De Boeck are acknowledged.

REFERENCES

1. K.-F. Berggren and B. E. Sernelius, *Phys. Rev. B* **24,** 1971 (1981).
2. J. Serre and A. Ghazali, *Phys. Rev. B* **28,** 4704 (1983).
3. P. Van Mieghem, *Rev. Mod. Phys.* (1991).
4. J. A. Del Alamo and R. M. Swanson. *IEEE Trans. Electron. Devices* **ED-31,** 1878 (1984); M. J. Kumar and K. N. Bhat, *IEEE Trans. Electron. Devices* **ED-36,** 1803 (1989).
5. J. W. Slotboom and H. C. de Graaff, *Solid-St. Electron.* **19,** 857 (1976).
6. Z. Yu and R. W. Dutton, *Sedan III—A Generalized Electronic Material Device Analysis Program*, Integrated Circuits Laboratory, Stanford University (1985).
7. M. Sugiyama, H. Takemura, C. Ogawa, T. Tashiro, T. Morikawa and M. Nakamae, *IEDM*, p. 221 (1989).
8. H. S. Bennett and J. R. Lowney, *Solid-St. Electron.* **33,** 675 (1990).
9. P. Van Mieghem, G. Borghs and R. Mertens, *Phys. Rev. B* **44,** 12,822 (1991).
10. V. Sayakanit and H. R. Glyde, *Phys. Rev. B* **22,** 6222 (1980).
11. B. I. Halperin and M. Lax, *Phys. Rev.* **148,** 722 (1966).
12. S. Noor Mohammad, *Solid-St. Electron.* **30,** 685 (1987).
13. See the Appendix of S. Noor Mohammad, *Solid-St. Electron.* **33,** 339 (1990).
14. See the Appendix of P. Van Mieghem, R. P. Mertens and R. J. Van Overstraeten, *J. appl. Phys.* **67,** 9 (1990).
15. J. C. S. Woo and J. D. Plummer, *IEDM*, p. 401 (1987).
16. J. D. Cressler, *Cryogenics* **30,** 1036 (1990).
17. H. De Man, R. Mertens and R. Van Overstraeten, *Electron. Lett.* **9,** 3rd May (1973).
18. J. J. H. Van Den Biesen, *Solid-St. Electron.* **29,** 529 (1986).
19. M. S. Lundstrom, M. E. Klausmeier-Brown, M. R. Melloch, R. K. Ahrenkiel and B. M. Keyes, *Solid-St. Electron.* **33,** 693 (1990).